AIP | Applied Physics Letters

Frequency-swept time-reversed ultrasonically encoded optical focusing

Yuta Suzuki and Lihong V. Wang

Citation: Applied Physics Letters **105**, 191108 (2014); doi: 10.1063/1.4901955
View online: http://dx.doi.org/10.1063/1.4901955
View Table of Contents: http://scitation.aip.org/content/aip/journal/apl/105/19?ver=pdfcov
Published by the AIP Publishing

Frequency-swept time-reversed ultrasonically encoded optical focusing

Yuta Suzuki and Lihong V. Wang[a)]
Optical Imaging Laboratory, Department of Biomedical Engineering, Washington University in St. Louis, St. Louis, Missouri 63130, USA

(Received 14 September 2014; accepted 5 November 2014; published online 11 November 2014)

A technique to rapidly scan an optical focus inside a turbid medium is attractive for various biomedical applications. Time-reversed ultrasonically encoded (TRUE) optical focusing has previously demonstrated light focusing into a turbid medium, using both analog and digital devices. Although the digital implementation can generate a focus with high energy, it has been time consuming to scan the TRUE focus inside a sample. Here, by sweeping the frequencies of both ultrasound and light, we demonstrate a multiplex recording of ultrasonically encoded wavefronts, accelerating the generation of multiple TRUE foci. Using this technique, we obtained a 2-D image of a fluorescent target centered inside a turbid sample having a thickness of 2.4 transport mean free paths. © *2014 AIP Publishing LLC*. [http://dx.doi.org/10.1063/1.4901955]

Fluorescence imaging is widely used to obtain biological images by scanning an optical focus.[1] However, due to scattering, optical focusing using an ordinary lens is limited to shallow depths of one transport mean free path, or 1 l_t' ($\sim$1 mm in human skin),[2] beyond which scattering both reduces the amount of light arriving at the target and blurs the resulting image.

One way to overcome this limitation is to use time-reversed ultrasonically encoded (TRUE) focusing.[3,4] In TRUE focusing, a focused ultrasonic (US) pulse, applied inside a turbid sample, frequency modulates (or encodes) light within the acoustic volume. A phase-conjugated version of the encoded wavefront is then generated, using either analog or digital phase conjugate mirrors (PCMs).[3–6] Digital PCMs, consisting of a camera and a spatial light modulator (SLM), are attractive for higher energy focusing.[4–6] To record the encoded wavefront, a reference beam interferes with the encoded light on the camera, causing the intensity of the interferogram to beat at their difference frequency.[6] The encoded wavefront is extracted from the beat, and then its phase-conjugated version is reproduced using the SLM. Upon back-propagation to the sample, the phase-conjugated beam forms an optical focus at the original location of the ultrasound volume.

It has been previously shown that TRUE focusing improves the resolution, thereby allowing deep fluorescence imaging beyond 1 l_t' inside a scattering medium.[4–6] However, one of the challenges of applying digital TRUE focusing for imaging was the long time (several seconds) taken to generate a single optical focus.[5,6] The low signal-to-noise ratio (SNR) of the encoded-light detection typically mandates that multiple frames of interferograms be recorded and averaged to obtain a single encoded wavefront.

Here, we propose a method called frequency-swept TRUE focusing, which takes advantage of the multiple recorded frames used for encoded-light detection to accelerate TRUE focal scanning. By sweeping the frequency of both the ultrasound and the light at the same time, we achieve simultaneous recording of multiple wavefronts, corresponding to different positions along the acoustic axis, without sacrificing SNR and using the same number of camera frames. A similar concept was previously demonstrated in Ref. 7, which used two US pulses of different frequencies for wavefront recording. The use of two US pulses allowed two TRUE foci to be generated from a single recording, thereby reducing the recording time by half. Here, we show that, by recording many more holograms in the same amount of time, frequency-swept TRUE focusing increases the number of foci generated after a single recording stage.

Frequency sweeping was previously used in ultrasound-modulated optical tomography to improve the acoustic axial resolution.[8] Here, we use a similar concept to obtain multiple holograms within a single recording stage. As shown in Fig. 1(a), a frequency-swept US pulse is sent through the scattering sample. The US frequency at a point y along the acoustic axis at time t is given by

$$f_{US}(y,t) = a_{US} + b(t - y/v_{US}), \tag{1}$$

where a_{US} is the initial US frequency, b is the rate at which the frequency is swept, and v_{US} is the speed of sound within the medium. After a brief delay (t_0) to allow the ultrasound to propagate, a laser beam then illuminates the sample, with its optical frequency swept at the same rate. The optical frequency at time t is given by

$$f_L(t) = a_L + b(t - t_0), \tag{2}$$

where a_L is the initial optical frequency. Inside the sample, the US beam frequency modulates the diffusively propagating light. The down-modulated (i.e., encoded) light frequency is given by

$$f_E(y) = f_L(t) - f_{US}(y,t) = (a_L - a_{US}) + b(y - v_{US}t_0)/v_{US}. \tag{3}$$

When the encoded light is mixed with a reference beam with frequency $f_R = a_L - a_{US}$, the frequency of the optical beat observed by the camera is given by

[a)]Electronic mail: lhwang@wustl.edu.

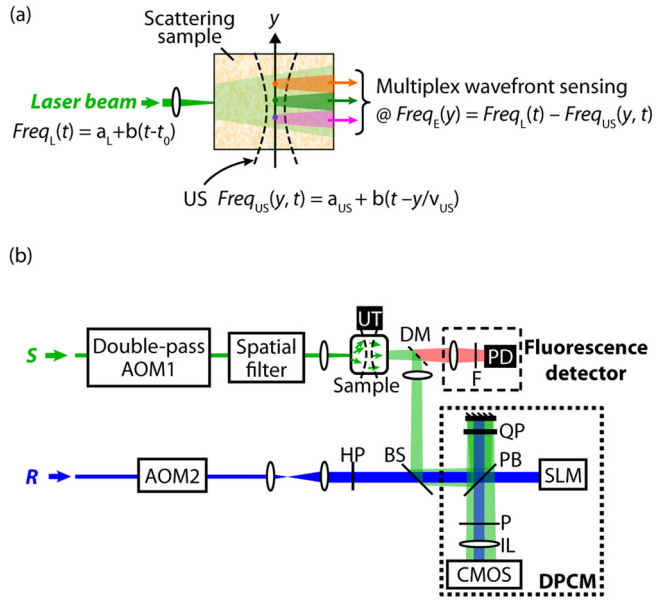

FIG. 1. Schematic illustration of the concept and implementation of frequency-swept TRUE. (a) Multiplex wavefront sensing using frequency-swept ultrasound and light. (b) Implementation of frequency-swept TRUE focusing system. AOM, acousto-optic modulator; BS, beamsplitter; CMOS, CMOS camera; DM, dichroic mirror; DPCM, digital phase-conjugate mirror; F, color filter; HP, half-wave plate; IL, imaging lens; P, polarizer; PB, polarizing beamsplitter; PD, photodiode; QP, quarter-wave plate; R, reference beam; S, sample beam; SLM, spatial light modulator; UT, ultrasonic transducer.

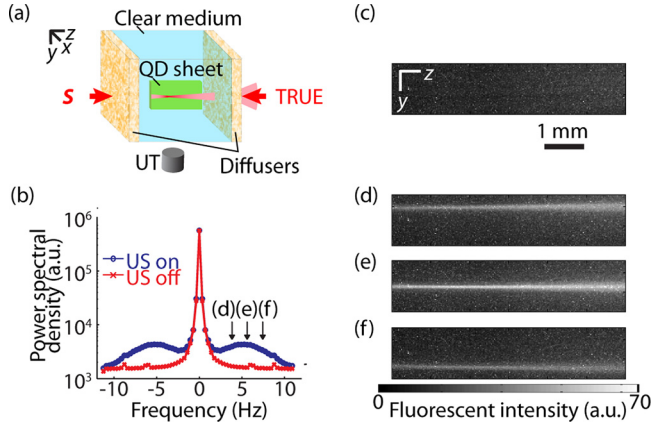

FIG. 2. Observation of multiple TRUE foci generated after a single recording stage. (a) Schematic illustration of the sample configuration. (b) Encoded signal spectrum after a single recording stage. (c) Fluorescent pattern excited using a flat phase pattern on SLM. (d)–(f) Fluorescent patterns excited showing the generated TRUE foci by using phase maps from different encoded-frequency components, which are indicated in Fig. 2(b).

$$f_B(y) = f_E(y) - f_R = b(y - v_{US}t_0)/v_{US}. \quad (4)$$

As seen in Eq. (4), the optical beat is composed of multiple frequencies, corresponding to different depths inside the sample along the y axis. From the measured intensity variation along the time axis, Fourier decomposition allows us to calculate the phases of the beats at each frequency, giving the desired wavefronts. Thus, frequency-sweeping can be used to record multiple wavefronts emanating from different locations at once, and to generate TRUE foci at multiple locations.

Our implementation of frequency-swept TRUE focusing is illustrated schematically in Fig. 1(b). The output of a 3.5 W continuous-wave laser (Verdi V-10, Coherent) was split into two beams: a vertically polarized sample beam (S) and a horizontally polarized reference beam (R). An acousto-optic modulator (AOM1) was used to sweep the S beam frequency. Because the spatial mode of S (i.e., the optical speckle pattern inside the scattering sample) must not change during the recording time, AOM1 was in a double-pass configuration to avoid angular deflection.[9] After AOM1, a spatial filter, comprised of a 25-μm pinhole and a confocal lens pair, ensured that the optical mode was unchanged while S illuminated the scattering sample. To demonstrate the proof-of-concept, we used a sample consisting of a thin fluorescent sheet suspended in a clear gelatin medium (water:gelatin = 90:10 wt. %) placed between two ground-glass diffusers, as shown in Fig. 2(a). To make the fluorescent sheet, we dispersed quantum dots (QD, Ocean Nanotech, QSA-600-2) in a gelatin solution. A frequency-swept US beam modulated the diffusively propagating light inside the sample. R was frequency-shifted by +120 MHz by AOM2, and was then expanded to fill the aperture of the SLM. The two beams were then recombined using a beamsplitter before being directed to the digital PCM, as indicated by the dotted block in Fig. 1(b). In the digital PCM, a mirror was placed at the symmetrical plane to the SLM (PLUTO, Holoeye) about a polarizing beamsplitter (PB). R and the diffuse light from the sample formed interferograms on the mirror, which was imaged by a CMOS camera (pco.Edge, PCO) to capture the diffuse wavefront. The polarization of R was tuned by using a half-wave plate, so that a small portion was reflected by the PB to generate the interferogram. The SLM and the CMOS camera were 1:1 pixel matched. The SLM curvature was measured using a Michelson interferometer, and was corrected for in the experiment.[10]

During the recording stage, a focused US transducer (Olympus NDT, V324-SU) emitted 800-ns US pulses repeatedly every 30 μs into the sample. The focal length of the US transducer was 14 mm. When the US pulse reached the focal zone of the transducer, AOM1 and AOM2 (AOM-802AF1, IntraAction) were turned on simultaneously to generate 1 μs optical pulses of S and R. The US frequency was swept from 12.5 to 37.5 MHz throughout the recording time of 2.84 s. The sweep rate was therefore $b = 8.80$ MHz/s. The frequency of S was also swept from +132.5 to +157.5 MHz at the same rate as the ultrasound. After propagating through the sample, S interfered with R at the CMOS camera in the digital PCM. The camera exposure time was 31 ms, therefore each interferogram was integrated over 1034 optical pulses. At a frame rate of 22.5 Hz, 64 interferograms were captured. To obtain the wavefronts, the argument of the spectral density at the beat frequencies, measured at each CMOS pixel, was extracted by discrete Fourier transformation (DFT). The measured power spectrum, averaged over the CMOS pixels after a single recording stage, is shown in Fig. 2(b). As expected, when the frequency-swept ultrasound was turned on, we observed a broadband signal increase over the baseline case without ultrasound.

In the readout stage, as soon as the SLM displayed the phase-conjugated wavefront, R was turned on to read out the displayed wavefront. To observe the propagation of the

phase-conjugated light inside the sample, a CCD camera imaged the fluorescent excitation on the QD sheet placed between two diffusers. When a flat pattern was displayed on the SLM, the imaged fluorescent excitation did not show a focused beam (Fig. 2(c)), due to random scattering by the ground glass. In contrast, for the frequency-swept TRUE, a clear focused beam is seen, as shown in Figs. 2(d)–2(f). The corresponding frequency values were 3.9 Hz, 5.6 Hz, and 7.4 Hz, respectively, as indicated in Fig. 2(b). We see that the TRUE focus was translated vertically as the SLM sequentially displayed phase-conjugated wavefronts calculated from the beat of different frequencies. Theoretically, the acoustic-axial resolution dy is given by $dy = v_{US}/w$, where v_{US} is the acoustic speed in the sample medium and w is the range of the frequency sweep. To see this, let us note that dy is the acoustic propagation distance during the frequency-sweep time across the frequency resolution df of the DFT in the wavefront calculation, i.e., $dy = v_{US} \times df/b$. Given the frequency sweep rate b and the total recording time $1/df$, we have $w = b/df$. Therefore, $dy = v_{US}/w$. In our experiment, we chose $w = 25$ MHz, and v_{US} was quantified from the US pulse-echo signal to be 1.6 mm/μs, which agrees with the reported value;[11] therefore, we estimated dy as 64 μm.

As a comparison, we also performed ordinary TRUE focusing (i.e., without frequency-sweep) using the same sample. We used single cycle US pulses at 25 MHz to match the US pulse length to the theoretical axial resolution for frequency-swept TRUE focusing. To minimize US pulse propagation during the sample illumination, the S and R pulse durations were set to 0.16 μs, the shortest times achievable using the AOMs. The intensities of both S and R were increased to match the camera exposure used in frequency-swept TRUE focusing. The frequency difference of the R and S beams was chosen so that the CMOS camera observed a 5.6 Hz optical beat between R and the encoded light. The CMOS camera again captured 64 frames of the interferograms. Fig. 3(a) shows the averaged power spectra acquired with and without the ultrasound, calculated in the same way as for Fig. 2(b). Unlike in Fig. 2(b), the encoded signal was observed only at the 5.6 Hz beat frequency. The measured SNR of the encoded signal was 3.0, which was comparable to the SNR of 2.7 observed at the same beat frequency in Fig. 2(b). Note that without frequency sweeping, only a single TRUE focus can be generated (Fig. 3(b)). These data confirm that frequency-swept TRUE focusing is faster, as focusing at different locations using the ordinary method would require the recording process to be repeated.

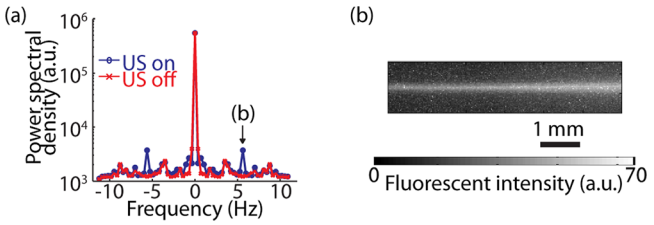

FIG. 3. TRUE focusing without frequency sweeping. (a) Encoded signal spectrum after a single recording stage. (b) Fluorescent pattern excited by using the phase map from the encoded signal.

Moreover, the SNR of the recordings is similar for both methods.

To experimentally quantify the resolution of frequency-swept TRUE focusing, we measured the edge spread function of a TRUE focus centered inside a turbid sample having a total thickness of $2\,l_t'$, which is shown in Fig. 4(a). The turbid medium was made by mixing intralipid into clear gel-medium (water:gel:intralipid = 89:10:1 wt. %). We embedded a rectangular fluorescent target at the mid-plane of the sample, as shown in Fig. 4(b). To measure the edge spread function, we used the representative spectral component at 5.6 Hz to form a TRUE focus, chosen because of its relatively high encoded-signal level, as seen in Fig. 2(b). By mechanically translating the sample in both x and y directions, we measured the fluorescent signal at each sample position. A photodiode measured the excited fluorescence from the sample, after passing through a dichroic mirror and a long-pass filter as shown in Fig. 1(b). We subtracted the fluorescent signal due to the background diffuse light, which originated from incomplete phase conjugation due to the limited number of SLM pixels. The background fluorescence was measured using a phase map synthesized by alternatingly adding 0 and π rad in 5×5 blocks across the phase-conjugated wavefront.[5] The SLM displayed the phase-conjugated wavefront for 100 ms, and subsequently displayed the background phase map for 400 ms. The photodiode signal was band-pass filtered between 1 to 30 Hz, and then amplified by five times (SR560, SRS). The signal was averaged for 16 times using an oscilloscope.

The measured edge-spread functions along the x and y axes are shown in Figs. 4(c) and 4(d), respectively. The x and y resolutions were quantified by fitting the measured data to the standard error function. The measured x-resolution was 220 μm, which agrees well with the US-focal full-width at half-maximum of 200 μm. On the other hand, we observed a widened y-resolution of 100 μm, compared with the theoretical value of 64 μm. The widening could be due to the envelope of the beat signals, caused by the spectral response of the US transducer and the S-beam intensity change due to AOM1 as the frequency is swept, which

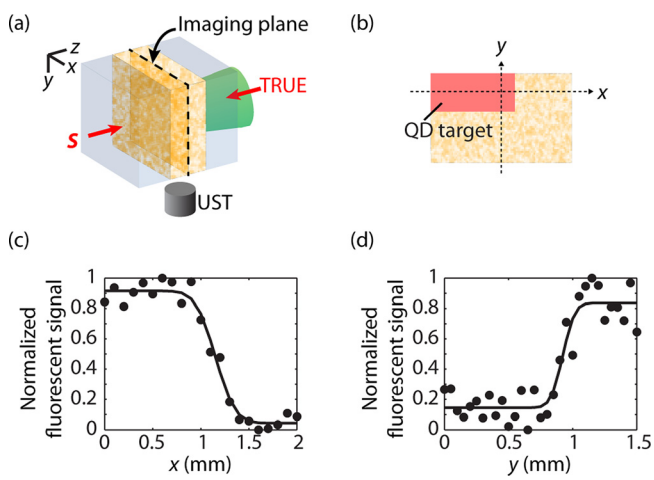

FIG. 4. Resolution measurement of frequency-swept TRUE focusing. (a) Sample configuration. (b) Schematic illustration of quantum-dot target placed at imaging plane inside the sample. (c) Measured edge-spread function in x direction. (d) Measured edge-spread function in y direction.

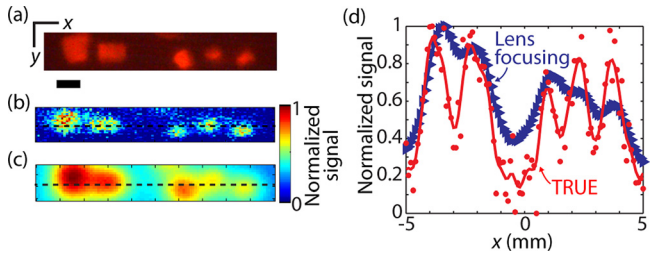

FIG. 5. Fluorescent images acquired by frequency-swept TRUE focusing. (a) Photo of fluorescent targets placed at the mid-plane of the sample, without a front turbid medium. Scale bar, 1 mm. (b) Image obtained by the proposed method. (c) Image obtained by displaying a flat phase pattern on the SLM. (d) Line plots along the dashed lines in (b) and (c), presented together with fitted curves.

results in a broadening of each beat frequency component. Error also is introduced in wavefront calculation because of the frequency resolution of DFT. Nevertheless, we note that frequency-swept TRUE focusing was still able to generate optical foci with substantially improved resolution, over optical focusing using an ordinary lens.

To further demonstrate the imaging capability of our system, we replaced the sample with one containing five fluorescent targets embedded inside a turbid medium having a total thickness of 2.4 l_t'. A photograph of the fluorescent objects, taken without the front turbid layer, is shown in Fig. 5(a). To obtain a 2-D image, we mechanically translated the sample in the x direction and at each stop performed frequency-swept TRUE focusing to scan an optical focus along the y-axis. We used 23 phase patterns from a single recording to scan the TRUE focus, corresponding to 23 pixels along the y-axis in the resulting image. Adaptive background subtraction was again used to measure the net fluorescent signal due to a TRUE focus. The resulting fluorescent image is shown in Fig. 5(b). We compared the image obtained using our method with an image obtained by mechanically scanning the sample while focusing light using an ordinary lens, as shown in Fig. 5(c). The cross-sectional plots along the dashed lines in Figs. 5(b) and 5(c) are shown in Fig. 5(d), together with a curve fitted by low-passing it using the measured x-resolution. We see that our system resolved five fluorescent targets, while optical focusing using an ordinary lens did not.

In our experiment, the range of the frequency sweep, and hence the resolution, was limited by both the spectral response of the acousto-optic diffraction efficiency, and the bandwidth of the US transducer. To sweep the optical frequency over a wider range, frequency-tunable optical sources can be used, as in Ref. 8. Together with a US transducer having a broader bandwidth, the acoustic-axial resolution of TRUE focus could be further improved. Also, the resolution can be improved by using higher frequency transducers, which have smaller focal volumes.

Currently, the speed of wavefront acquisition is mainly limited by the calculation time (several seconds) of the Fourier spectra from many ($\sim 2 \times 10^6$) camera pixels. By using a faster computer or dedicated computation devices (such as field-programmable gate arrays), we may accelerate the wavefront-calculation time. Further, faster image sensors, e.g., 500 fps for the used resolution of 1080×1920, can be used to accelerate the recording stage. By implementing these improvements, we may potentially reduce the wavefront acquisition time to less than 200 ms, which may be applicable for *in vivo* biological imaging experiments.[12]

In summary, we have proposed and demonstrated frequency-swept TRUE focusing, which allowed us to perform multiplexed wavefront sensing. By obtaining a y-axial 1-D image after a single recording stage, the system imaged fluorescent targets embedded in a thick turbid medium. Frequency-swept TRUE focusing is a promising step towards speeding up the generation and scanning of a TRUE focus inside a turbid medium, which is attractive for biological imaging applications.

We thank J. Ballard and J. W. Tay for editing the manuscript. This work was sponsored in part by National Institutes of Health grants DP1 EB016986 (NIH Director's Pioneer Award). L.W. has a financial interest in Microphotoacoustics, Inc. and Endra, Inc., which, however, did not support this work.

[1]B. A. Flusberg, A. Nimmerjahn, E. D. Cocker, E. A. Mukamel, R. P. J. Barretto, T. H. Ko, L. D. Burns, J. C. Jung, and M. J. Schnitzer, Nat. Methods **5**, 935 (2008).
[2]V. Ntziachristos, Nat. Methods **7**, 603 (2010).
[3]X. Xu, H. L. Liu, and L. V. Wang, Nat. Photonics **5**, 154 (2011).
[4]P. Lai, Y. Suzuki, X. Xu, and L. V. Wang, Laser Phys. Lett. **10**, 075604 (2013).
[5]Y. M. Wang, B. Judkewitz, C. A. DiMarzio, and C. Yang, Nat. Commun. **3**, 928 (2012).
[6]K. Si, R. Fiolka, and M. Cui, Nat. Photonics **6**, 657 (2012).
[7]R. Fiolka, K. Si, and M. Cui, Opt. Express **20**, 24827 (2012).
[8]G. Yao, S. Jiao, and L. V. Wang, Opt. Letters **25**, 734 (2000).
[9]E. A. Donley, T. P. Heavner, F. Levi, M. O. Tataw, and S. R. Jefferts, Rev. Sci. Instrum. **76**, 063112 (2005).
[10]J. Oton, P. Ambs, M. S. Millan, and E. Perez-Cabre, Appl. Opt. **46**, 5667 (2007).
[11]T. J. Hall, M. Bilgen, M. F. Insana, and T. A. Krouskop, IEEE Trans. Ultrason., Ferroelectr., Freq. control **44**, 1355 (1997).
[12]M. Cui, E. J. McDowell, and C. Yang, Opt. Express **18**, 25 (2010).